VOLUME 76 SEPARATE No. 12

PROCEEDINGS

AMERICAN SOCIETY
OF
CIVIL ENGINEERS

APRIL, 1950

INFLUENCE CHARTS FOR CONCRETE PAVEMENTS

By Gerald Pickett and G. K. Ray, Jun. ASCE

AIR TRANSPORT DIVISION

Headquarters of the Society
33 W. 39th St.
New York 18, N.Y.

PRICE $0.50 PER COPY

The Society is not responsible for any statement made or opinion expressed in its publications

---

Published at Prince and Lemon Streets, Lancaster, Pa., by the American Society of Civil Engineers. Editorial and General Offices at 33 West Thirty-ninth Street, New York 18, N. Y.

AMERICAN SOCIETY OF CIVIL ENGINEERS

Founded November 5, 1852

PAPERS

INFLUENCE CHARTS FOR CONCRETE PAVEMENTS

By Gerald Pickett[1] and G. K. Ray,[2] Jun. ASCE

Synopsis

Influence charts are presented for the purpose of obtaining theoretical deflections and moments of pavement slabs under load. The charts are similar to, and are used in the same manner as, those presented by Nathan M. Newmark, M. ASCE, for the determination of theoretical stresses and displacements in elastic foundations.

Points at a slab edge, points near a slab edge, and points far from any slab edge are considered. Both the assumption of a subgrade modulus as originally proposed by H. M. Westergaard, M. ASCE, and the assumption of a deep elastic solid considered by Mr. Westergaard and others are treated. The charts are based on the theoretical equations derived by Mr. Westergaard and by A. H. A. Hogg.

Introduction

In deriving the basic equations for the stresses and deflections that occur in concrete pavements,[3] Mr. Westergaard used the assumption that the subgrade reaction per unit of area at any point is proportional to the slab deflection at that point. He has often stated that this assumption was "only an empirical makeshift justified by usable results." In his 1933 paper,[4] he introduced a correction in regard to the subgrade reaction to be applied to his formulas for interior loading for cases in which the load could be assumed to be uniformly distributed over a circular area. The object of this correction was to obtain formulas more nearly in accord with tests on concrete pavements for highways. Mr. Westergaard gave this matter further attention in his 1939 paper[5] which

Note.—Written comments are invited for publication; the last discussion should be submitted by September 1, 1950.

[1] Prof. of Applied Mechanics, Kansas State College, Manhattan, Kans.; formerly Research Physicist, Portland Cement Assn., Chicago, Ill.

[2] Engr., Highways and Municipal Bureau, Portland Cement Assn., Chicago, Ill.

[3] "Om Beregning af Plader paa elastisk Underlag med saerlight Henblik paa Spørgsmaalet om Spaendinger i Betonveje," by H. M. Westergaard, *Ingenioren*, Vol. 32, 1923, pp. 513–524.

[4] "Analytical Tools for Judging Results of Structural Tests of Concrete Pavements," by H. M. Westergaard, *Public Roads*, December, 1933, pp. 185–188.

[5] "Stresses in Concrete Runways of Airports," by H. M. Westergaard, *Proceedings*, Highway Research Board, National Research Council, Vol. 19, 1939, pp. 199–200.

dealt specifically with concrete runways for airports. He made a "plausible estimate" of what the correction should be to bring his formula for maximum stress for interior loading into agreement with what would be obtained if the assumed subgrade had been replaced by a "deep elastic solid." As far as is known, he has not prepared corrective terms applicable to other shapes of loaded areas or to stresses near the slab boundaries.

In 1938, Mr. Hogg[6] and D. L. Holl,[7] independently, solved the problem of a thin slab of infinite size supported by a semi-infinite elastic solid (corresponding to the deep elastic solid mentioned by Mr. Westergaard). Mr. Hogg expressed his formulas in series form, and made a few numerical computations.

From a study of experimental data, especially those obtained by the Swedish State Road Institute, S. G. Bergstrom[8] concluded that the subgrade acts more nearly like a semi-infinite solid (the assumption used by Mr. Hogg) than like a dense liquid (the assumption used by Mr. Westergaard when the corrective term is not used). Mr. Bergstrom, therefore, based all his calculations on the assumption of an elastic solid subgrade. However, being unable to obtain an exact mathematical solution for the cases of interest to him, Mr. Bergstrom used a method of approximation, and obtained numerical results for the case of a circular slab under a centrally applied load.

Most investigators believe that, of the two types of subgrade, the behavior of the semi-infinite elastic solid more nearly represents actual subgrade performance. Support for this belief is furnished by data from bearing tests with various sizes of circular bearing plates, such as those reported by L. A. Palmer and J. B. Thompson.[9] The constant C, characteristic of a solid subgrade, when computed from the data, is practically independent of the diameter of the bearing plate, as it should be, whereas the constant k, characteristic of a liquid subgrade, when computed from the data is found to be approximately inversely proportional to the diameter of the plate. In determining these constants from the load-deflection data, the following formulas are used:

$$k = \frac{q}{w} \qquad (1a)$$

and

$$C = \frac{q\,d}{w} \qquad (1b)$$

in which q is the unit load; d is the diameter of the plate; and w is the settlement of the plate.

On the other hand, because of variation of the subgrade material with depth, one cannot be certain that the behavior of a subgrade under a large slab can be predicted from its behavior under a much smaller bearing plate. In this connection, it can be shown that if the subgrade were an elastic solid layer of finite thickness, and were supported by a base of much more rigid material,

[6] "Equilibrium of a Thin Plate, Symmetrically Loaded, Resting on an Elastic Foundation of Infinite Depth," by A. H. A. Hogg, *Philosophical Magazine*, Series 7, Vol. 25, 1938, pp. 576–582.

[7] "Thin Plates on Elastic Foundation," by D. L. Holl, *Proceedings*, 5th International Cong. for Applied Mechanics, Cambridge, Mass., 1938, John Wiley & Sons, Inc., New York, N. Y., 1939, pp. 71–74.

[8] "Circular Plates with Concentrated Load on an Elastic Foundation," by S. G. Bergstrom, *Bulletin No. 6*, Swedish Cement and Concrete Research Inst., Stockholm, 1946.

[9] "Pavement Evaluation by Loading Tests at Naval and Marine Corps Air Stations," by L. A. Palmer and J. B. Thompson, *Proceedings*, Highway Research Board, National Research Council, Vol. 27, 1947, pp. 125–143.

then for bearing plates of diameters larger than the thickness of the elastic layer, the effect of the subgrade on the bearing plate would be more nearly like that of a dense liquid than that of a semi-infinite elastic solid. However, if smaller bearing plates were used on this elastic layer, the effect would be more like an elastic solid than a dense liquid.

It is beyond the scope of this paper to discuss the merits of either assumption further. It is the primary purpose of this paper to extend the work of Messrs. Westergaard and Hogg by presenting solutions of their equations in the form of influence charts. (Influence charts were prepared by Mr. Newmark in 1942 and 1947 to simplify calculations for similar problems.[10,11]) Although these charts may be used for any rigid type of pavement of uniform thickness, it is believed they will be used chiefly in connection with airport pavements. They greatly facilitate the determination of theoretical deflections and moments caused by loads on pavement slabs. In fact, with the charts one may readily obtain these values for any distribution of load that might be transmitted by airplane landing gears. It is only necessary to:

(1) Draw the imprint of tire or tires on transparent paper to a scale that depends on the properties of the slab and its supporting subgrade.

(2) Place the drawing on the appropriate chart in a position that depends on the location of the load with respect to the point for which values are desired; and

(3) Count the blocks of the chart covered by the diagram.

The value desired is then obtained as a product of the intensity of loading, a factor expressing properties of subgrade and slab, and the number of blocks covered by the diagram.

Eight influence charts were prepared from the basic equations of Messrs. Westergaard and Hogg.[11a] These charts were for both moments and deflections for four different cases. The cases are classified according to the point for which values may be determined and according to the subgrade assumption, as follows:

(1) Interior—liquid subgrade
(2) Interior—solid subgrade
(3) Edge—liquid subgrade
(4) One half of the radius of relative stiffness from an edge—liquid subgrade

Only the one case of solid subgrade was treated because it was the only one for which a basic formula was available at the time this project was under way. However, subsequently, the problem of an infinite slab on an elastic solid layer of finite thickness which in turn is supported by a rigid base and the problem of a finite rectangular slab on an elastic solid of infinite depth have been solved, and influence charts for these conditions have been prepared. No one should conclude that the writers favor a given subgrade assumption because they prepared influence charts for that assumption. Only after an adequate number

[10] "Influence Charts for Computation of Stresses in Elastic Foundations," by N. M. Newmark, *Bulletin No. 338*, Univ. of Illinois Eng. Experiment Station, Urbana, Ill., 1942.

[11] "Influence Charts for Computation of Vertical Displacements in Elastic Foundations," by N. M. Newmark, *Bulletin No. 367*, Univ. of Illinois Eng. Experiment Station, Urbana, Ill., 1947.

[11a] More detailed information on the use and application of these influence charts will be mailed free on request. Address the Portland Cement Assn., 33 West Grand Avenue, Chicago 10, Ill.

of charts or similar computational aids have been prepared for various assumptions and theoretical values based on these assumptions have been compared with a sufficient amount of reliable experimental data can it be said definitely that one assumption more nearly represents subgrade performance under pavement slabs than does another assumption.

Computations Preliminary to Preparation of Charts

The fundamental equations by Messrs. Westergaard and Hogg that formed the basis of the work will be given, followed by a general description of the computational procedure used. Certain tabulated summaries of the results will also be presented, but details of the work will be omitted. The following fundamental equations for deflection were used:

Interior—Liquid Subgrade.[12]—

$$w = \frac{P\,l^2}{4\,D}\,\mathrm{Re}\,H^1{}_0\left(\sqrt{i}\,\frac{r}{l}\right) \qquad (2)$$

Interior—Solid Subgrade.[13]—

$$w = \frac{P\,l^2}{8\,D}\sum_{m=0,1}^{\infty}(-1)^m\left\{\frac{\dfrac{8}{3\sqrt{3}}\left(\dfrac{r}{2\,l}\right)^{6m}}{[(3\,m)!]^2} + \frac{\dfrac{4}{\pi}\left[\log\frac{\lambda\,r}{2\,l} - \left(1+\tfrac{1}{2}+\cdots\frac{1}{3\,m+1}\right)\right]\left(\dfrac{r}{2\,l}\right)^{6m+2}}{[(3\,m+1)!]^2} - \frac{\dfrac{8}{3\sqrt{3}}\left(\dfrac{r}{2\,l}\right)^{6m+4}}{[(3\,m+2)!]^2} + \frac{2\left(\dfrac{r}{2\,l}\right)^{6m+5}}{[\Gamma\,(3\,m+3.5)]^2}\right\} \qquad (3)$$

Edge—Liquid Subgrade.[14]—

$$w = \frac{2\,P}{\pi\,k\,l^2}\int_0^{\infty}\frac{\gamma\cos\dfrac{\alpha\,x}{l}\left[\cos\dfrac{\beta\,y}{l} + (1-\mu)\,\alpha^2\sin\dfrac{\beta\,y}{l}\right]e^{-\gamma y/l}\,d\alpha}{1+4\,(1-\mu)\,\alpha^2\,\gamma^2-(1-\mu)^2\,\alpha^4} \qquad (4)$$

Near an Edge—Liquid Subgrade.[15]—

$$w_{II} = \frac{2\,P}{\pi\,k\,l^2}\int_0^{\infty}\frac{\gamma\cos\dfrac{\alpha\,x}{l}\left(A\cos\dfrac{\beta\,y}{l} + B\sin\dfrac{\beta\,y}{l}\right)e^{-\gamma y/l}\,d\alpha}{1+4\,(1-\mu)\,\alpha^2\,\gamma^2-(1-\mu)^2\,\alpha^4} \qquad (5)$$

$$w_I = w'_{II} + \frac{P}{\pi\,k\,l^2}\int_0^{\infty}\frac{\cos\dfrac{\alpha\,x}{l}}{\beta^2+\gamma^2}\left(\beta\cos\frac{\beta\,y}{l}\sinh\frac{\gamma\,y}{l} - \gamma\sin\frac{\beta\,y}{l}\cosh\frac{\gamma\,y}{l}\right)d\alpha \qquad (6)$$

[12] "Stresses in Concrete Runways of Airports," by H. M. Westergaard, *Proceedings*, Highway Research Board, National Research Council, Vol. 19, 1939, pp. 200 and 201, Eqs. 33 and 34.

[13] "Equilibrium of a Thin Plate, Symmetrically Loaded, Resting on an Elastic Foundation of Infinite Depth," by A. H. A. Hogg, *Philosophical Magazine*, Series 7, Vol. 25, 1938, p. 581, Eq. 13.

[14] "New Formulas for Stresses in Concrete Pavements of Airfields," by H. M. Westergaard, *Transactions*, ASCE, Vol. 113, 1948, p. 434, Eq. 36.

[15] "Om Beregning af Plader paa elastisk Underlag med saerlight Henblik paa Spørgsmaalet om Spaendinger i Betonveje," by H. M. Westergaard, *Ingenioren*, Vol. 32, 1923, p. 523, Eqs. 62 and 63.

Notation

The symbols used in the preceding equations and in subsequent equations in the text, unless adequately defined at place of occurrence, are defined as follows:

w = deflection:
- w_I = deflection in the region where y is negative;
- w_{II} = deflection in the region where y is positive;
- w'_{II} = same expression as w_{II} but applied to region where y is negative;

P = the concentrated load;

$D = \dfrac{E h^3}{12(1-\mu^2)}$ is the flexural rigidity of the slab;

h = slab thickness;

E = Young's modulus of slab;

μ = Poisson's ratio for slab, assumed to be 0.15 in all computations;

$l = \left(\dfrac{D}{k}\right)^{\frac{1}{4}} = \left[\dfrac{E h^3}{12(1-\mu^2)k}\right]^{\frac{1}{4}}$ for liquid subgrade;

$l = \left(\dfrac{2D}{C}\right)^{\frac{1}{4}}$ for solid subgrade;

k = weight density of assumed liquid subgrade;

C = rigidity of assumed solid subgrade (equal to $E/(1-\mu^2)$ in which E and μ are elastic constants of an elastic solid);

Re = "the real part of";

Im = "the imaginary part of";

H^1_0 = the Hankel function of zero order that vanishes for an infinite positive imaginary argument;

r, θ = polar coordinates;

x, y = rectangular coordinates;

λ = 1.781072—is the antilogarithm of Euler's constant;

$\Gamma(\ )$ = a gamma function;

$$\beta = \sqrt{\frac{\sqrt{1+\alpha^4}-\alpha^2}{2}};$$

$$\gamma = \sqrt{\frac{\sqrt{1+\alpha^4}+\alpha^2}{2}};$$

$$A = \frac{1}{2}\left\{1 + 2\gamma^2 g - (1-\mu)^2\alpha^4 + \left[1 + (1-\mu)^2\alpha^4 + g\sin\frac{2\beta c}{l} - 2\gamma^2 g\cos\frac{2\beta c}{l}\right]e^{-2\gamma c/l}\right\};$$

$$B = \frac{1}{2}\left[2(1-\mu)\alpha^2 - g + \left(2\gamma^2 g\sin\frac{2\beta c}{l} + g\cos\frac{2\beta c}{l}\right)e^{-2\gamma c/l}\right];$$

$$g = \frac{\mu\alpha^2}{2(\gamma^2+\beta^2)}[2\gamma^2 - (1-\mu)\alpha^2] + \frac{3(1-\mu)\alpha^2}{2} - \gamma^2; \text{ and}$$

c = distance from x-axis to the edge of the slab.

In Eqs. 2 to 6, w is the deflection due to a concentrated load P at the origin of coordinates. Eqs. 5 and 6 are essentially like those presented by Mr. Westergaard in 1923.[15] Eq. 5 reduces to Eq. 4 for c equal to zero; that is, A becomes unity, and B becomes equal to $(1 - \mu)\ \alpha^2$.

Eq. 6 is particularly interesting because the integrand of the integral expression oscillates with increasing amplitude as the variable α increases. However, when this integrand is combined with that of w'_{II}, the sum of the two oscillates about the α-axis with decreasing amplitude. Therefore, the question of evaluating "divergent integrals" need not arise in any discussion of Eq. 6 or of any subsequent formulas based on it.

CHART I

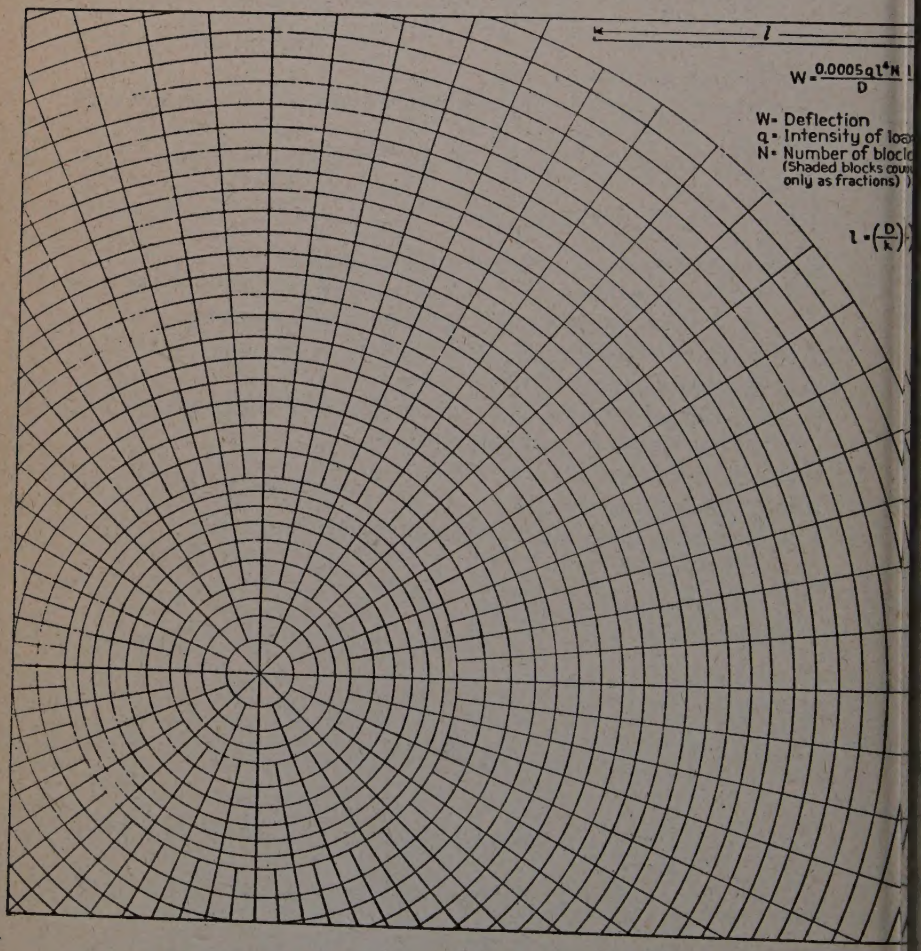

(*a*) Subgrade Assumed to Be a Dense Liquid

FIG. 1.—INFLUENCE CHART FOR DEFLECTION, $w = 0.0005\ \frac{q\ l^4}{D}\ N$, AT AN

Deflections from Distributed Loads

From Maxwell's reciprocal relations, each of the equations for deflection may also be considered to be the deflection at the origin caused by a concentrated load at the variable coordinate points. Then, by use of the principle of superposition and by integration, one may find the deflection at the origin due to a distributed load. For example, if P in Eq. 2 is replaced by $q\,r\,dr\,d\theta$, and is integrated with respect to r from 0 to a, and with respect to θ from θ_1 to θ_2, the result is

$$w = \frac{q\,l^4}{D}\left(\frac{\theta_2 - \theta_1}{2\,\pi}\right)\left[1 + \frac{\pi}{2}\frac{a}{l}\,\mathrm{Im}\,\sqrt{i}\,H^1{}_1\left(\frac{\sqrt{i}\,a}{l}\right)\right] \quad \ldots\ldots\ldots (7)$$

CHART 3

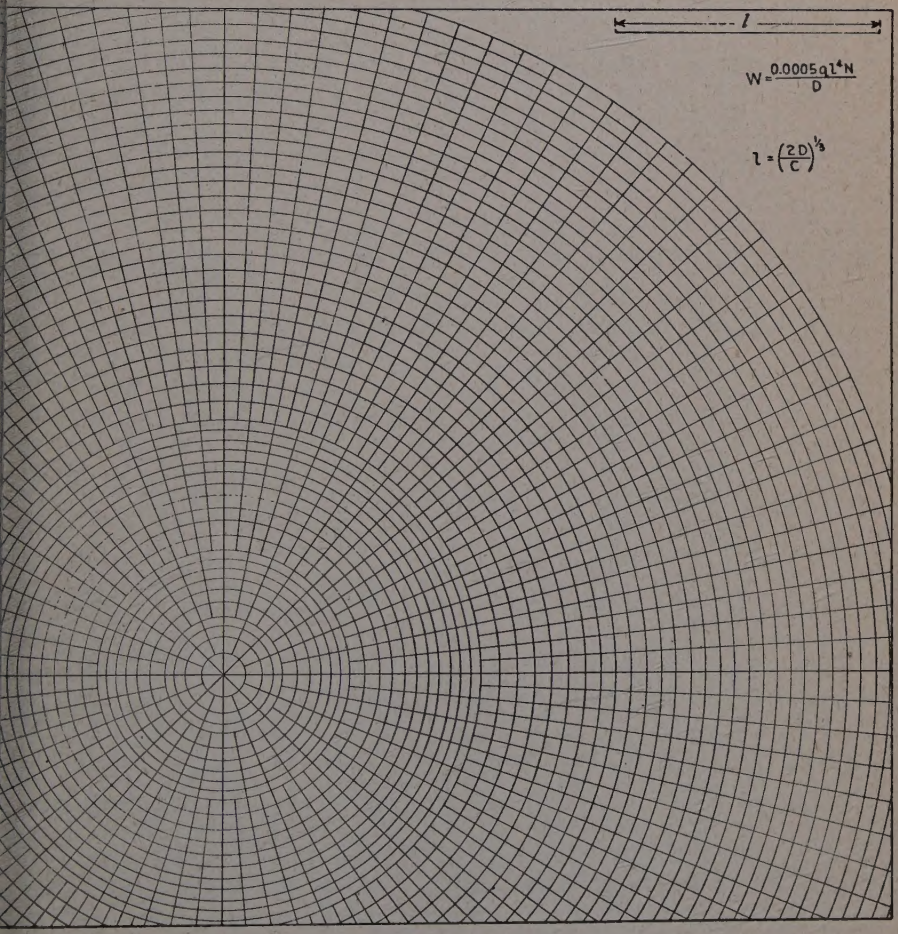

(*b*) Subgrade Assumed to Be an Elastic Solid

ior Point of a Concrete Slab (Poisson's Ratio for Concrete, 0.15)

TABLE I.—Deflection of Slab When Loaded in the Interior; Values of the Radii of Arcs Enclosing Given Numbers of Blocks N in the First Quadrant of the Appropriate Design Chart

(*a*) Liquid Subgrade; Fig. 1(*a*)						(*b*) Solid Subgrade; Fig. 1(*b*)							
No. (N)	$\frac{a}{l}$	No. (N)	$\frac{a}{l}$	No. (N)	$\frac{a}{l}$	No. (N)	$\frac{a}{l}$	No. (N)	$\frac{a}{l}$	No. (N)	$\frac{a}{l}$	No. (N)	$\frac{a}{l}$
(1)	(2)	(1)	(2)	(1)	(2)	(1)	(2)	(1)	(2)	(1)	(2)	(1)	(2)
0	0	94	0.750	270	1.463	0	0	110	0.6273	398	1.2837	782	1.9609
2	0.1012	110	0.821	286	1.524	2	0.0815	126	0.6744	430	1.3442	814	2.0146
6	0.1762	126	0.890	302	1.592	6	0.1414	142	0.7192	462	1.4037	846	2.0681
10	0.2285	142	0.957	318	1.659	10	0.1829	158	0.7620	494	1.4621	878	2.1215
14	0.2707	158	1.021	334	1.727	14	0.2167	174	0.8031	526	1.5197	910	2.1747
22	0.3424	174	1.085	350	1.797	22	0.2726	190	0.8428	558	1.5765	942	2.2277
30	0.4032	190	1.148	366	1.870	30	0.3193	206	0.8812	590	1.6328	974	2.2810
38	0.4566	206	1.211	382	1.945	38	0.3604	222	0.9186	622	1.6885	1,006	2.3343
46	0.5057	222	1.273	398	2.023	46	0.3976	238	0.9550	654	1.7436	1,038	2.3874
54	0.5516	238	1.336	414	2.105	54	0.4320	270	1.0253	686	1.7984	1,070	2.4406
62	0.5946	254	1.399	430	2.192	62	0.4641	302	1.0930	718	1.8529	1,102	2.4938
78	0.675	....	....	....	....	78	0.5232	334	1.1583	750	1.9070	1,134	2.5470
....	....	....	....	....	....	94	0.5771	366	1.2218	....	....	....	....

CHART 5

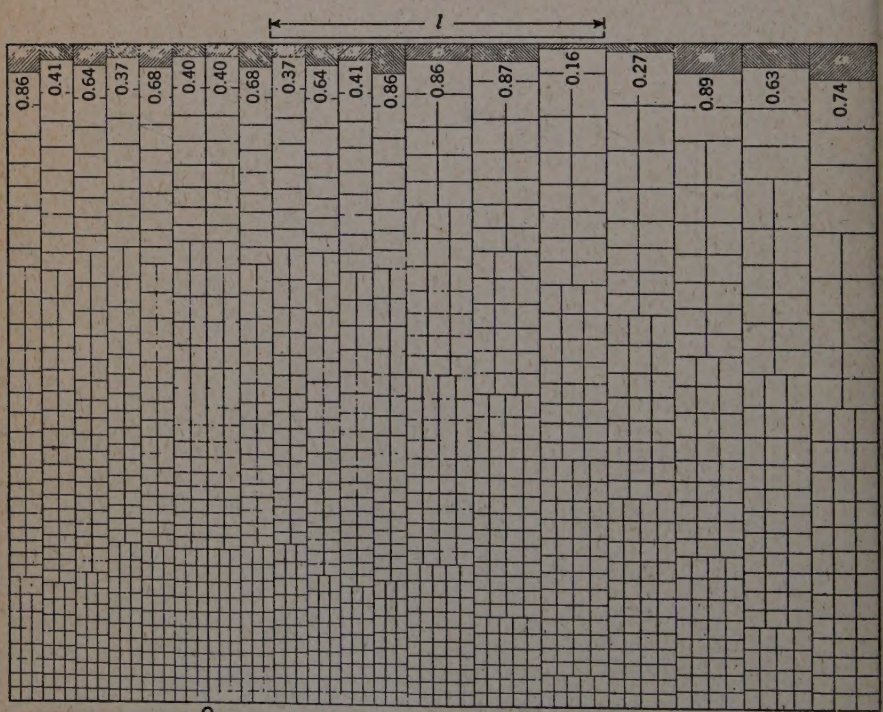

$$W=\frac{0.0005qL^4N}{D} \qquad l=\left(\frac{D}{k}\right)^{\frac{1}{4}}$$

(*a*) Deflection at the Edge

Fig. 2.—Influence Chart for the Deflection, $w=0.0005\frac{ql^4}{D}N$, at Point O, Due to a Poisson's Ratio for Concrete, 0.15; and

In the preparation of Table 1(a) from which chart 1 (Fig. 1) was constructed, the quantity in brackets in Eq. 7 was set equal to 0.0005 times given integers and the resulting equations were solved by trial for a/l. The given integers determine the number of blocks to be enclosed by each circle of chart 1. Eq. 3 treated in like manner resulted in Table 1(b) from which chart 3 was constructed.

Tables 2(a) and 3(a), which form the basis for the two charts in Fig. 2 were prepared by use of a slightly different procedure. (Table 2(a) is similar to that introduced by Mr. Westergaard in 1926.[16]) In each of Eqs. 4, 5, and 6, the load P was replaced by the load $q\,dx\,dy$, then integrated with respect to x between a_1 and a_2, and with respect to y between b_1 and b_2—that is, the numbers of blocks for given regions of charts 5 and 7 (Fig. 2) were determined rather than

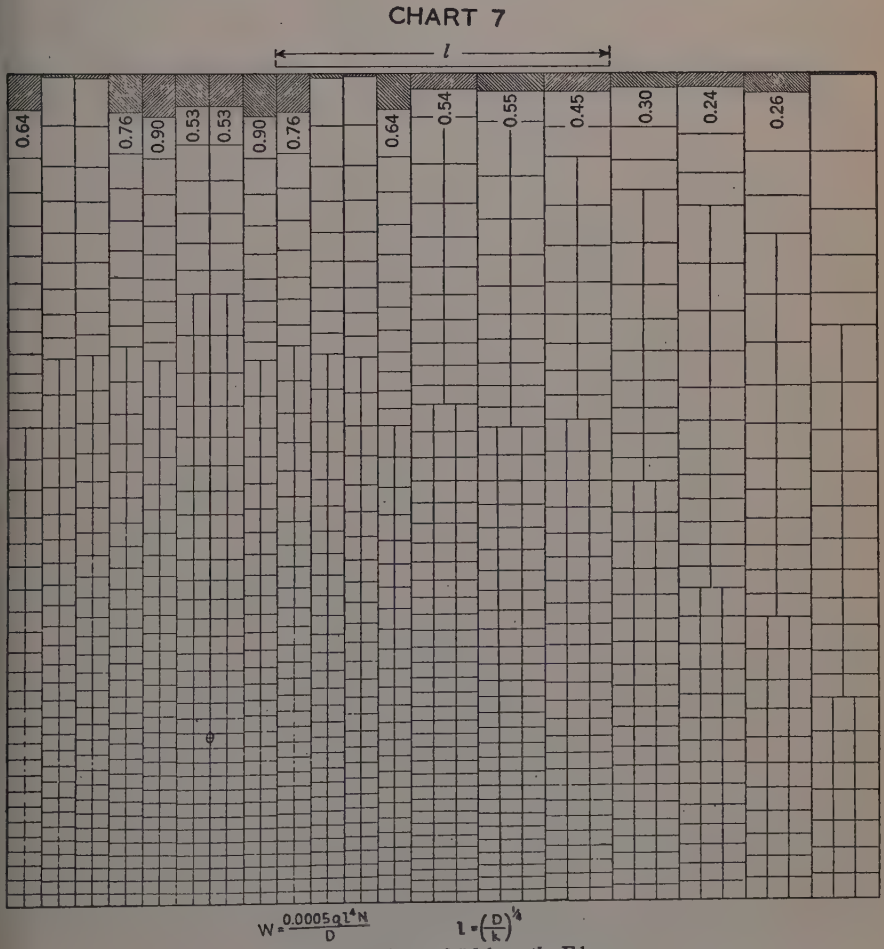

(b) Deflection at 0.5 l from the Edge

LOAD NEAR THE EDGE OF A CONCRETE SLAB (SUBGRADE ASSUMED TO BE A DENSE LIQUID; SHADED BLOCKS COUNT ONLY AS FRACTIONS)

[16] "Stresses in Concrete Pavements Computed by Theoretical Analysis," by H. M. Westergaard, *Public Roads*, April, 1926, pp. 29 and 30, Figs. 8 and 9.

the boundaries of a given group of blocks as was done for the two charts in Fig. 1. The previous method of solving by trial was not feasible here because of the nature of the equations involved.

TABLE 2.—DEFLECTIONS AND MOMENTS AT THE EDGE OF A CONC OF AREA FOR THE RE

$\frac{b^{(a)}}{l}$	(a) DEFLECTION AT POINT O, FIG. 2(a)												
	RANGE OF RATIOS,[b] a/l:												
	0	0.1	0.2	0.3	0.4	0.5	0.6	0.8	1.0	1.2	1.4	1.6	1.8
2.0	1.086	1.082	1.05	1.02	1.013	0.97	0.92	0.85	0.757	0.63	0.505	0.41	0.3
1.8	1.281	1.271	1.259	1.234	1.20	1.17	1.16	1.02	0.88	0.76	0.64	0.505	0.4
1.6	1.728	1.718	1.696	1.663	1.61	1.53	1.47	1.33	1.18	1.03	0.86	0.724	0.5
1.4	2.267	2.254	2.230	2.183	2.128	2.05	1.951	1.78	1.60	1.37	1.177	1.00	0.8
1.2	2.969	2.92	2.859	2.807	2.737	2.64	2.503	2.281	2.032	1.77	1.529	1.30	1.0
1.0	3.669	3.644	3.595	3.528	3.432	3.33	3.14	2.848	2.543	2.218	1.923	1.65	1.3
0.8	4.547	4.514	4.449	4.353	4.207	4.07	3.85	3.490	3.111	2.733	2.356	2.00	1.6
0.6	5.285	5.244	5.161	5.046	4.89	4.69	4.433	4.009	3.563	3.13	2.700	2.316	1.9
0.5	5.807	5.759	5.67	5.532	5.36	5.17	4.857	4.381	3.895	3.406	2.94	2.525	2.1
0.4	6.374	6.314	6.20	6.05	5.861	5.63	5.267	4.754	4.222	3.701	3.196	2.739	2.3
0.3	6.973	6.902	6.75	6.56	6.35	6.12	5.713	5.139	4.554	3.999	3.454	2.956	2.5
0.2	7.602	7.506	7.356	7.15	6.89	6.612	6.14	5.529	4.900	4.287	3.710	3.181	2.6
0.1	8.263	8.150	7.960	7.73	7.406	7.12	6.65	5.924	5.241	4.589	3.967	3.42	2.8
0.0													

[a] Symbol b denotes vertical distance from point O in Figs. 2 a

The result of integrations with respect to x and y was expressed in the form:

$$w = w(a_2, b_2) - w(a_1, b_2) - w(a_2, b_1) + w(a_1, b_1) \ldots\ldots\ldots (8)$$

in which the general term $w(a, b)$ is as follows:

$$w = \frac{2\,q\,l^4}{\pi\,D}\int_0^\infty \frac{\gamma^2\left[(A + 2\,B\,\beta^2)\left(1 - \cos\frac{\beta\,b}{l}\,e^{-\gamma b/l}\right) + (2\,A\,\beta^2 - B)\sin\frac{\beta\,b}{l}\,e^{-\gamma b/l}\right]\sin\frac{\alpha\,a}{l}}{\alpha\,(\gamma^2 + \beta^2)\,[1 + 4\,(1-\mu)\,\alpha^2\,\gamma^2 - (1-\mu)^2\,\alpha^4]}\,d\alpha \quad (9)$$

These integrals were evaluated as follows: The integrand of each integral was divided into two parts. The first part was arbitrarily taken in a form that could be integrated by standard procedures, and at the same time in a form that approached the total integrand as the variable α increased. The second part of the integrand was then integrated numerically using the trapezoidal rule.[17] For this purpose, this second part of the integrand was evaluated for values of

[17] "Higher Mathematics for Engineers and Physicists," by I. S. and E. S. Sokolnikoff, McGraw-Hill Book Co., Inc., New York, N. Y., 1941, p. 556.

α at 0.1 intervals in the range from 0 to 2.0 and at 0.5 intervals in the range from 2.0 to 5.0. In all cases, the second part was considered to be negligible for values of α in excess of 5.0.

AB RESTING ON A LIQUID SUBGRADE (NUMBER OF BLOCKS PER 0.01 l^2 DICATED IN THE APPROPRIATE CHART)

(b) MOMENT AT POINT O, FIG. 4(a)													$\frac{b^{(a)}}{l}$
RANGE OF RATIOS,[b] a/l:													
0.1	0.2	0.3	0.4	0.5	0.6	0.8	1.0	1.2	1.4	1.6	1.8	2.0	
13	3.0	3.0	2.9	2.7	2.4	1.92	1.33	0.74	0.19	−0.43	−0.6	−0.92	2.0
05	4.0	3.84	3.59	3.22	2.97	2.31	1.5	0.7	−0.07	−0.6	−0.9	−1.25	1.8
3	5.3	5.0	4.7	4.12	3.69	2.96	1.6	0.7	0.15	−0.8	−1.2	−1.7	1.6
99	6.75	6.51	5.99	5.4	4.75	3.4	2.0	0.85	−0.23	−1.0	−1.66	−2.26	1.4
15	8.90	8.39	7.67	6.8	5.9	4.3	2.48	0.89	−0.47	−1.3	−2.0	−2.5	1.2
14	11.71	10.87	9.84	8.26	7.1	5.0	2.62	0.5	−0.83	−2.0	−2.8	−3.5	1.0
27	15.51	14.19	12.36	10.42	8.3	5.5	2.53	0.13	−1.67	−2.80	−3.5	−4.03	0.8
64	19.45	17.29	14.5	11.94	9.2	5.81	2.08	−0.6	−2.3	−3.4	−4.2	−4.7	0.6
1	22.5	19.5	15.8	12.8	9.60	5.83	1.96	−0.8	−2.7	−3.8	−4.6	−5.0	0.5
81	26.08	21.74	17.20	13.19	9.72	5.6	1.54	−1.46	−3.2	−4.4	−5.0	−5.4	0.4
12	30.50	23.7	17.8	13.36	9.7	5.2	1.0	−1.8	−3.8	−4.9	−5.5	−5.9	0.3
86	35.5	25.0	18.1	13.13	9.4	4.72	0.3	−2.6	−4.4	−5.30	−6.1	−6.3	0.2
42	40.66	25.18	18.0	12.5	8.6	3.95	−0.6	−3.56	−5.2	−6.0	−6.5	−6.8	0.1
													0.0

mbol a denotes horizontal distance from point O in Figs. 2 and 4.

MOMENTS FROM DISTRIBUTED LOADS

Since moments have direction within the plane of the slab, and since Maxwell's reciprocal relations do not, in general, apply between loads and moments, the derivations of the equations to be used in connection with the preparation of influence charts for moments require special consideration. As the basic formulas for interior loading, Eqs. 2 and 3, are based on the assumption that the slab is of infinite extent in all radial directions, it follows that the deflection at point $(r - dr,\theta)$ due to a load P at the origin is equal to the deflection at point (r,θ) due to the same load at point (dr,θ). Then, by Maxwell's reciprocal relations between loads and deflections, it follows that the slope dw/dr at point (r,θ) due to a load P at the origin is equal to the negative of the slope dw/dr at the origin due to the same load at point (r,θ). By similar reasoning, the reciprocal relation may be extended to higher derivatives for a slab of infinite extent in all radial directions.

TABLE 3.—DEFLECTIONS AND MOMENTS AT POINT O, 0.5 l FROM [illegible] OF BLOCKS PER 0.01 l^2 OF AREA FOR [illegible]

$\frac{b}{l}$[a]	(a) DEFLECTION AT POINT O, FIG. 2(b)												
	RANGE OF RATIOS,[b] a/l:												
	0	0.1	0.2	0.3	0.4	0.5	0.6	0.8	1.0	1.2	1.4	1.6	1.8
2.0	0.705	0.700	0.691	0.677	0.660	0.639	0.599	0.539	0.470	0.398	0.324	0.252	0.1[illegible]
1.8	0.961	0.954	0.944	0.928	0.900	0.877	0.812	0.747	0.660	0.566	0.475	0.384	0.2[illegible]
1.6	1.169	1.168	1.140	1.122	1.097	1.057	0.999	0.901	0.787	0.680	0.563	0.455	0.3[illegible]
1.4	1.514	1.498	1.491	1.455	1.421	1.375	1.303	1.158	1.08	0.98	0.756	0.65	0.4[illegible]
1.2	1.877	1.865	1.839	1.804	1.756	1.702	1.589	1.459	1.278	1.114	0.937	0.776	0.6[illegible]
1.0	2.265	2.230	2.208	2.166	2.096	2.030	1.904	1.716	1.512	1.297	1.101	0.901	0.7[illegible]
0.8	2.771	2.767	2.74	2.67	2.591	2.497	2.348	2.118	1.881	1.613	1.431	1.183	0.9[illegible]
0.6	3.123	3.098	3.05	2.98	2.888	2.797	2.598	2.350	2.072	1.80	1.474	1.291	1.0[illegible]
0.5	3.380	3.351	3.295	3.216	3.114	2.992	2.813	2.519	2.227	1.933	1.655	1.388	1.1[illegible]
0.4	3.645	3.612	3.547	3.456	3.348	3.218	3.007	2.700	2.383	2.070	1.766	1.488	1.2[illegible]
0.3	3.910	3.870	3.799	3.696	3.574	3.437	3.207	2.880	2.542	2.213	1.896	1.598	1.3[illegible]
0.2	4.180	4.134	4.049	3.948	3.795	3.655	3.409	3.059	2.699	2.355	2.016	1.704	1.4[illegible]
0.1	4.436	4.383	4.290	4.159	4.036	3.868	3.606	3.237	2.866	2.486	2.139	1.810	1.5[illegible]
0	4.667	4.612	4.515	4.389	4.240	4.074	3.800	3.412	3.017	2.630	2.261	1.917	1.6[illegible]
−0.1	4.868	4.818	4.723	4.596	4.444	4.272	3.988	3.575	3.185	2.769	2.386	2.030	1.7[illegible]
−0.2	5.065	5.017	4.927	4.799	4.645	4.470	4.176	3.767	3.315	2.906	2.504	2.130	1.7[illegible]
−0.3	5.268	5.221	5.133	5.001	4.847	4.662	4.357	3.918	3.468	3.031	2.613	2.234	1.8[illegible]
−0.4	5.464	5.418	5.326	5.202	5.037	4.844	4.541	4.082	3.617	3.162	2.737	2.338	1.9[illegible]
−0.5													

[a] Symbol b denotes vertical distance from points O in Figs. 2 and[illegible]

The moment at point (r,θ) in a direction of the reference axis due to a load at the origin is given by

$$M = -\frac{D}{2}\left[(1+\mu)\left(\frac{d^2w}{dr^2}+\frac{1}{r}\frac{dw}{dr}\right)+(1-\mu)\left(\frac{d^2w}{dr^2}-\frac{1}{r}\frac{dw}{dr}\right)\cos 2\theta\right] \quad . . (10)$$

As a consequence of the foregoing reciprocal relations, Eq. 10 also represents the moment at the origin in the direction of the reference axis due to a load at point (r,θ) for a slab of infinite extent.

Substitute w from either Eqs. 2 or 3 into Eq. 10; let $P = q\,r\,dr\,d\theta$; and integrate r from 0 to a and θ from θ_1 to θ_2. The result is an expression for the moment M, in the direction of the reference axis, due to a load of intensity q uniformly distributed over a wedge bounded by $\theta = \theta_1$, $\theta = \theta_2$, and $r = a$. From the resulting expressions, Table 4 was prepared; and the two charts in Fig. 3 were then constructed from the information in the tables.

GE OF A CONCRETE SLAB RESTING ON A LIQUID SUBGRADE (NUMBER GION INDICATED ON THE APPROPRIATE CHART)

(b) MOMENT AT POINT O, FIG. 4(b) — RANGE OF RATIOS,[b] a/l:													$\frac{b^{(a)}}{l}$
0.1	0.2	0.3	0.4	0.5	0.6	0.8	1.0	1.2	1.4	1.6	1.8	2.0	
128	2.084	1.96	1.83	1.68	1.50	1.295	0.881	0.463	0.091	−0.264	−0.49	−0.711	2.0
796	2.737	2.628	2.473	2.239	2.083	1.658	1.098	0.559	0.062	−0.341	−0.642	−0.906	1.8
592	3.523	3.378	3.156	2.882	2.601	2.063	1.344	0.668	0.055	−0.446	−0.850	−1.090	1.6
782	4.661	4.431	4.120	3.732	3.251	2.544	1.566	0.658	−0.091	−0.679	−1.115	−1.380	1.4
132	5.967	5.638	5.25	4.65	4.0	3.035	1.785	0.683	−0.217	−0.903	−1.395	−1.718	1.2
964	7.697	7.191	6.500	5.7	4.9	3.516	1.919	0.589	−0.494	−1.25	−1.758	−2.2	1.0
415	9.85	9.0	8.1	7.0	5.8	3.95	1.9	0.4	−0.720	−1.65	−2.2	−2.65	0.8
394	12.1	11.0	9.5	7.7	6.25	4.1	1.9	0.25	−1.0	−1.9	−2.5	−3.0	0.6
3	13.8	12.2	10.2	8.075	6.364	4.173	1.8	0.0	−1.2	−2.1	−2.7	−3.25	0.5
1	15.9	13.281	10.7	8.3	6.4	4.05	1.6	−0.2	−1.4	−2.3	−2.95	−3.500	0.4
301	17.808	14.328	11.1	8.50	6.4	3.9	1.4	−0.4	−1.64	−2.5	−3.2	−3.70	0.3
350	20.132	15.042	11.234	8.55	6.5	3.8	1.2	−0.605	−1.86	−2.72	−3.4	−3.935	0.2
060	21.972	15.5	11.2	8.85	6.6	3.7	1.03	−0.74	−1.893	−2.874	−3.6	−4.274	0.1
856	22.536	16.3	11.8	9.3	6.9	3.8	1.0	−0.882	−2.066	−3.15	−3.9	−4.55	0
140	21.831	16.7	12.513	9.674	7.346	4.179	1.0	−1.016	−2.299	−3.308	−4.153	−4.8	−0.1
279	20.80	16.9	13.233	10.214	7.606	4.464	1.0	−1.1	−2.5	−3.5	−4.4	−5.0	−0.2
702	19.85	17.032	13.844	10.854	8.065	4.599	1.0	−1.25	−2.7	−3.75	−4.5	−5.1	−0.3
359	19.039	16.720	13.907	11.121	8.355	4.774	1.065	−1.4	−2.846	−3.889	−4.686	−5.209	−0.4
													−0.5

ymbol a denotes horizontal distance from points O, in Figs. 2 and 4.

In the basic formulas for loading at an edge or near an edge (Eqs. 4, 5, and 6), it is assumed that the slab extends indefinitely far in both the positive and the negative directions of x, indefinitely far in the positive direction of y, but only a finite distance c in the negative y-direction ($c = 0$ for Eq. 4). By a process of reasoning similar to that used previously, it may be shown that, for a slab with these boundaries, the following relations hold:

(1) The quantity $\frac{\partial^n w}{\partial x^n}$ at point (0,0) due to a load P at point (x,y) is equal to $\left(-\frac{\partial}{\partial x}\right)^n w$ at point (x,y) due to the same load at point (0,0).

(2) The quantity $\frac{\partial^n w}{\partial y^n}$ at point (0,0) due to a load P at point (x,y) is equal to $\left(\frac{\partial}{\partial c} - \frac{\partial}{\partial y}\right)^n w$ at point (x,y) due to the same load at point (0,0). There-

TABLE 4.—MOMENTS IN SLAB WHEN LOADED IN THE INTERIOR; LOCATION OF THE LINES BOUNDING THE BLOCKS OF THE FIRST QUADRANT OF THE APPROPRIATE DESIGN CHART (RADII, IN TERMS OF l, OF THE BOUNDING ARCS. EXCEPT WHERE NOTED, THE RADII OF CONSECUTIVE ARCS BETWEEN GIVEN RADIAL LINES ARE ARRANGED CONSECUTIVELY IN THE COLUMNS)

(*a*) SUBGRADE ASSUMED TO BE A DENSE LIQUID; FIG. 3(*a*)

Angles of Bounding Radii:

0°	5°	10°	15°	20°	25°	30°	35°	40°	45°	50°	55°	60°	65°	70°	75°	80°	85°	90°
0.0173																		
0.0332									0.0311									
0.0503									0.0478						0.0456			
0.0768			0.0753			0.0729			0.0704			0.0686			0.0675			
0.0986			0.0964			0.0930			0.0895			0.0868			0.0856			
0.1535	0.1530	0.1520	0.1505	0.1488	0.1468	0.1445	0.1423	0.1401	0.1378	0.1360	0.1342	0.1326	0.1312	0.1300	0.1292	0.1287	0.1284	
0.2011	0.2003	0.1987	0.1965	0.1938	0.1907	0.1876	0.1842	0.1809	0.1778	0.1748	0.1722	0.1698	0.1679	0.1663	0.1652	0.1644	0.1640	
0.2458	0.2445	0.2423	0.2392	0.2354	0.2311	0.2267	0.2222	0.2177	0.2136	0.2097	0.2063	0.2032	0.2006	0.1986	0.1970	0.1959	0.1953	
0.2888	0.2872	0.2842	0.2801	0.2752	0.2695	0.2637	0.2579	0.2523	0.2470	0.2422	0.2380	0.2342	0.2310	0.2284	0.2265	0.2253	0.2246	
0.3317	0.3296	0.3257	0.3202	0.3138	0.3066	0.2995	0.2923	0.2853	0.2788	0.2730	0.2677	0.2634	0.2597	0.2566	0.2544	0.2529	0.2521	
0.3748	0.3721	0.3671	0.3603	0.3521	0.3410	0.3345	0.3256	0.3172	0.3095	0.3026	0.2964	0.2910	0.2866	0.2831	0.2804	0.2787	0.2778	
0.4190	0.4156	0.4093	0.4006	0.3905	0.3792	0.3688[a]	0.3583[a]	0.3484[a]	0.3393[a]	0.3312[a]	0.3241[a]	0.3181[a]	0.3131[a]	0.3091[a]	0.3060[a]	0.3040[a]	0.3030[a]	
0.4651	0.4608	0.4527	0.4418	0.4294	0.4140	0.5078	0.4877	0.4701	0.4543	0.4407	0.4291	0.4192	0.4112	0.4048	0.3999	0.3969	0.3954	
0.5140	0.5084	0.4980	0.4844	0.4690	0.4532	0.6584	0.6224	0.5926	0.5676	0.5467	0.5292	0.5160	0.5033	0.4944	0.4881	0.4838	0.4816	
0.5670	0.5596	0.5461	0.5288	0.5090	0.4900	0.8423[a]	0.7732	0.7233	0.6843	0.6534	0.6286	0.6089	0.5931	0.5810	0.5722	0.5665	0.5637	
0.6263	0.6179	0.5984	0.5760	0.5511	0.5294[a]	0.894	0.9616[a]	0.8705	0.8092	0.7643	0.7297	0.7031	0.6822	0.6664	0.6552	0.6477	0.6442	
0.6964	0.6844	0.6567	0.6270	0.5985	0.7019	0.958	1.019	1.0523[a]	0.9489	0.8825	0.8348	0.7991	0.7720	0.7521	0.7378	0.7285	0.7240	
0.7903	0.7642	0.7251	0.6835	0.6457	0.9577[a]	1.040	1.082	1.102	1.1160	1.0127	0.9461	0.8985	0.8641	0.8386	0.8210	0.8097	0.8042	
0.9660[b]	0.9073	0.8167	0.7490	0.6969	1.1288	1.1699	1.169	1.161	1.3425[a]	1.1628	1.0668	1.0036	0.9591	0.9275	0.9056	0.8916	0.8849	
1.171	0.9815[b]	1.0115[b]	0.8311	0.7563	1.210[b]	1.3198[b]	1.3136	1.235	1.425	1.3477	1.2018	1.1160	1.0591	1.0192	0.9925	0.9755	0.9674	
1.254	1.1850	1.2201	0.9716	0.8280	1.4360	1.5560	1.4557[b]	1.3385	1.530	1.6212[a]	1.3588	1.2387	1.1648	1.1151	1.0821	1.0619	1.0522	
1.320	1.2718	1.3057	1.0591[b]	0.9163	1.5322	1.6592	1.7065	1.518	1.709	1.736	1.5565	1.3770	1.2788	1.2167	1.1760	1.1511	1.1395	
1.377	1.3376	1.3717	1.2704	1.1364[b]	1.6054	1.7382	1.8166	1.6220[b]	1.8220[b]	1.921	1.8500[a]	1.5379	1.4041	1.3247	1.2747	1.2445	1.2304	
1.426	1.3945	1.4306	1.3586	1.3424	1.6710	1.8069	1.9027	1.8939	2.1239	2.0645[b]	1.970	1.7390	1.5450	1.4420	1.3799	1.3432	1.3263	
1.472	1.4452	1.4836	1.4263	1.4345	1.7304	1.8690	1.9775	2.01345			2.174	2.0309[a]	1.7096	1.5713	1.4933	1.4484	1.4278	
1.516	1.4921	1.5312	1.4866	1.5041	1.7856	1.9259	2.0449				2.3455[b]	2.144	1.9137	1.7179	1.6172	1.5611	1.5363	
1.555	1.5347	1.5748	1.5410	1.5666	1.8334	1.9793						2.298	2.2014[a]	1.8899	1.7553	1.6850	1.6541	
1.592	1.5750	1.6152[a]	1.5900	1.6228	1.8795	2.0298						2.6622[b]		2.1035	1.9138	1.8226	1.7836	
1.630	1.6135	1.7627	1.6347[a]	1.6737[a]	1.9232									2.4050[a]	2.1030[a]	1.9800	1.9291	
1.664[a]	1.6495[a]	1.8920	1.7930	1.8447	1.9661											2.1658[a]	2.0970[a]	
1.793	1.7840	2.0108[a]	1.9308	1.9959[a]	2.0091													
1.909	1.9043		2.0260[a]															
2.019[a]	2.0167[a]																	

TABLE 4.—(*Continued*)

(*b*) SUBGRADE ASSUMED TO BE AN ELASTIC SOLID; FIG. 3(*b*)

Angles of Bounding Radii:

0°	5°	10°	15°	20°	25°	30°	35°	40°	45°	50°	55°	60°	65°	70°	75°	80°	85°	90°
←									0.0173									→
←									0.0332									→
←									0.0478									→
←									0.0704									→
←									0.0895									→
←			0.0503															→
←			0.0768			0.0753			0.0729						0.0685			→
←			0.0985			0.0964			0.0929						0.0868			→
←															0.0456			→
←															0.0311			→
←																0.0675		→
←																0.0854		→

0.1535	0.1529	0.1519	0.1504	0.1487	0.1467	0.1445	0.1423	0.1400	0.1379	0.1360	0.1341	0.1325	0.1312	0.1301	0.1292	0.1287	0.1284
0.2009	0.2001	0.1986	0.1964	0.1937	0.1906	0.1874	0.1840	0.1807	0.1776	0.1748	0.1721	0.1698	0.1679	0.1664	0.1652	0.1644	0.1640
0.2451	0.2441	0.2418	0.2387	0.2351	0.2310	0.2265	0.2220	0.2175	0.2134	0.2097	0.2062	0.2032	0.2007	0.1987	0.1971	0.1961	0.1956
0.2878	0.2866	0.2835	0.2794	0.2746	0.2692	0.2634	0.2576	0.2519	0.2466	0.2420	0.2377	0.2340	0.2309	0.2284	0.2266	0.2253	0.2246
0.3306	0.3289	0.3246	0.3192	0.3130	0.3061	0.2989	0.2917	0.2847	0.2783	0.2727	0.2675	0.2631	0.2594	0.2564	0.2542	0.2527	0.2519
0.3726	0.3704	0.3655	0.3588	0.3510	0.3426	0.3337[a]	0.3249[a]	0.3164[a]	0.3087	0.3022	0.2961	0.2908	0.2865	0.2830	0.2804	0.2787	0.2778
0.4158	0.4131	0.4069	0.3986	0.3890	0.3787	0.4701	0.4531	0.4383	0.3384[a]	0.3309[a]	0.3238[a]	0.3178[a]	0.3128[a]	0.3088[a]	0.3058[a]	0.3038[a]	0.3029[a]
0.4601	0.4568	0.4491	0.4389	0.4270	0.4147	0.6114	0.5821	0.5573	0.4527	0.4392	0.4278	0.4182	0.4104	0.4042	0.3996	0.3966	0.3951
0.5055	0.5015	0.4923	0.4799	0.4655	0.4509	0.7686	0.7198	0.6796	0.5635	0.5438	0.5269	0.5130	0.5019	0.4930	0.4866	0.4823	0.4801
0.5546	0.5497	0.5380	0.5266	0.5050	0.4876	0.9642[a]	0.8760	0.8127	0.6764	0.6480	0.6240	0.6051	0.5903	0.5785	0.5700	0.5645	0.5617
0.6089	0.6026	0.5870	0.5678	0.5458	0.5250	1.0307	1.0699[a]	0.9612	0.7951	0.7545	0.7213	0.6964	0.6777	0.6624	0.6516	0.6449	0.6413
0.6699	0.6617	0.6403	0.6152	0.5879	0.5634	1.1037	1.1297	1.1386[a]	0.9226	0.8657	0.8211	0.7885	0.7653	0.7459	0.7328	0.7242	0.7196
0.7392	0.7286	0.6990	0.6674	0.6324	0.6030	1.1941	1.1975	1.1907	1.0644	0.9843	0.9274	0.8855	0.8537	0.8294	0.8137	0.8031	0.7975
0.8183	0.8045	0.7640	0.7262	0.6802	0.6442	1.3309	1.2773	1.2482	1.2297	1.1133	1.0375	0.9820	0.9443	0.9141	0.8952	0.8825	0.8757
1.0150	0.9206	0.8460	0.7838	0.7312	0.6865	1.5067[b]	1.3795	1.3108	1.4355[a]	1.2577	1.1552	1.0862	1.0373	0.9997	0.9782	0.9627	0.9544
1.0545[b]	1.0733[b]	0.9691	0.8588	0.7873	0.7316	1.7833	1.5479	1.3821	1.4990	1.4260	1.2836	1.1947	1.1342	1.0907	1.0628	1.0448	1.0349
1.2767	1.2984	1.0988[b]	0.9582	0.8505	0.7804	1.8972	1.6936[b]	1.4659	1.5730	1.6350[a]	1.4261	1.3106	1.2355	1.1840	1.1498	1.1285	1.1166
1.3652	1.3892[a]	1.3407	1.1694[b]	0.9258	0.8332	1.9970	1.9971	1.5726	1.6555	1.7551	1.5894	1.4365	1.3426	1.2806	1.2397	1.2147	1.2003
1.4383[a]	1.6430	1.4331	1.4052	1.0256	0.8916	2.0850	2.1328	1.7393	1.7638	1.7859[a]	1.5751	1.4569	1.3861	1.3331	1.3038	1.2886
1.6667	1.8257	1.5115	1.4997	1.2516[b]	0.9586	2.1629	2.2417	1.9364[b]	1.8876	1.8430	1.8426	1.7314	1.5804	1.4888	1.4308	1.3961	1.3794
1.8372	1.9815	1.5807[a]	1.5818	1.4941	1.0395	2.2330	2.3356	2.2774	2.1765	1.9316	1.9025	1.9124[a]	1.7150	1.6025	1.5334	1.4929	1.4732
1.9879	2.1230	1.7915	1.6534[a]	1.5941	1.1510	2.2976	2.4216	2.4357	2.2560[b]	2.0372	1.9679	1.9630	1.8647	1.7251	1.6421	1.5942	1.5715
2.1255	2.2559	1.9624	1.8726	1.6809	1.3623[b]	2.3587	2.5022			2.1749	2.0400	2.0163	2.0346	1.8582	1.7580	1.7014	1.6747
2.2545	2.3829	2.1144	2.0511	1.7566[a]	1.6210	2.4190				2.3900	2.1192	2.0724	2.2329	2.0050	1.8828	1.8155	1.7842
2.3783	2.5063[a]	2.2556	2.2106	1.9885	1.7258	2.4807					2.2080	2.1321	2.4738[a]	2.1694	2.0185	1.9379	1.9009
2.4986[a]		2.3902	2.3594	2.1785	1.8175	2.5380					2.3109	2.1961	2.5444	2.3574[a]	2.1675	2.0700	2.0259
		2.5201[a]	2.5016[a]	2.3496	1.8977[a]						2.4352	2.2649		2.4093	2.3342	2.2148	2.1617
				2.5099[a]	2.1472							2.3388		2.4633	2.5222[a]	2.3750[a]	2.3104
					2.3542							2.4203		2.5195	2.5733	2.4179	2.4753[a]
					2.5429[a]							2.5135				2.4620	2.5197
																2.5077	

[a] Values tabulated in the columns between superior letters *a* apply to every fourth arc only. Values for intermediate arcs may be found by interpolation. [b] Boundary between positive and negative blocks.

CHART 2

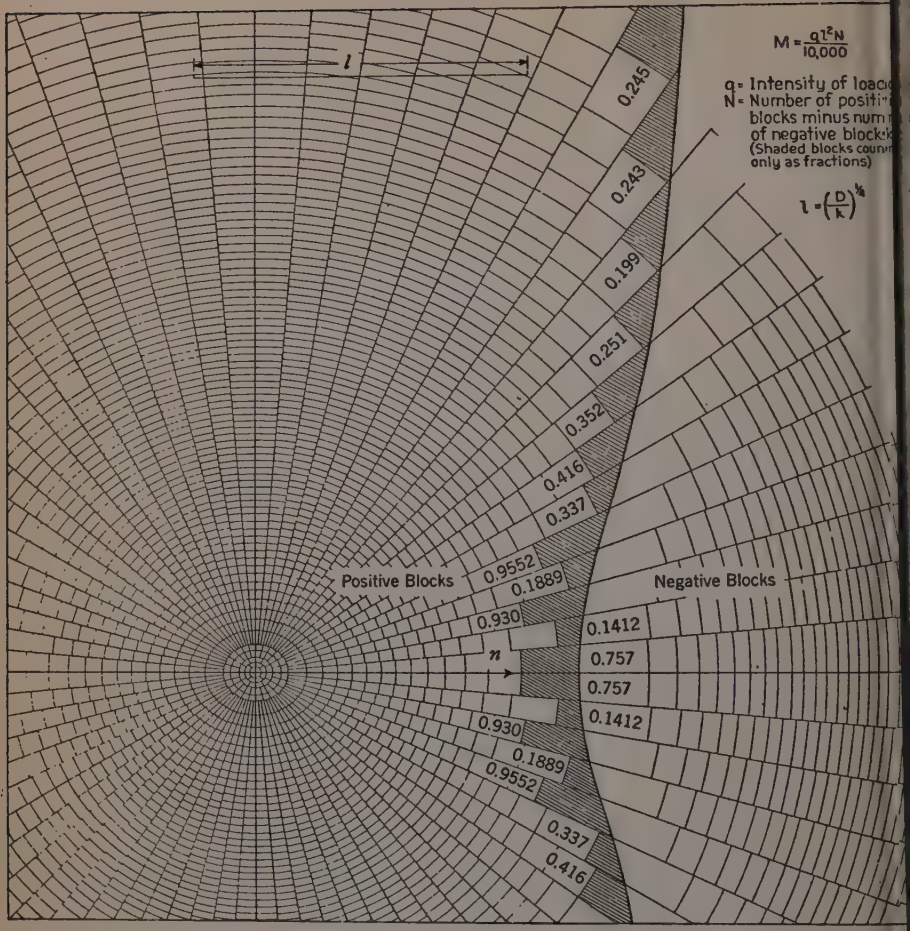

(a) Subgrade Assumed to Be a Dense Liquid

FIG. 3.—INFLUENCE CHARTS FOR THE MOMENT $M_x = \frac{q l^2 N}{10{,}000}$ IN THE INTERIOR OF THE BLOCKS; AND POISSON

fore, since $M_x = -D\left(\frac{\partial^2 w}{\partial x^2} + \mu \frac{\partial^2 w}{\partial y^2}\right)$, it follows that the moment M_x at point (0,0) due to a load at point (x,y) is given by

$$M_x = -D\left[\frac{\partial^2 w}{\partial x^2} + \mu\left(\frac{\partial^2 w}{\partial y^2} - 2\frac{\partial^2 w}{\partial y\, \partial c} + \frac{\partial^2 w}{\partial c^2}\right)\right] \ldots\ldots\ldots (11)$$

in which w is the deflection at point (x,y) due to the same load at point (0,0).

The expressions for deflection from Eqs. 4, 5, and 6 were each substituted into Eq. 11; P was placed equal to $q\,dx\,dy$ and the result was integrated with

CHART 4

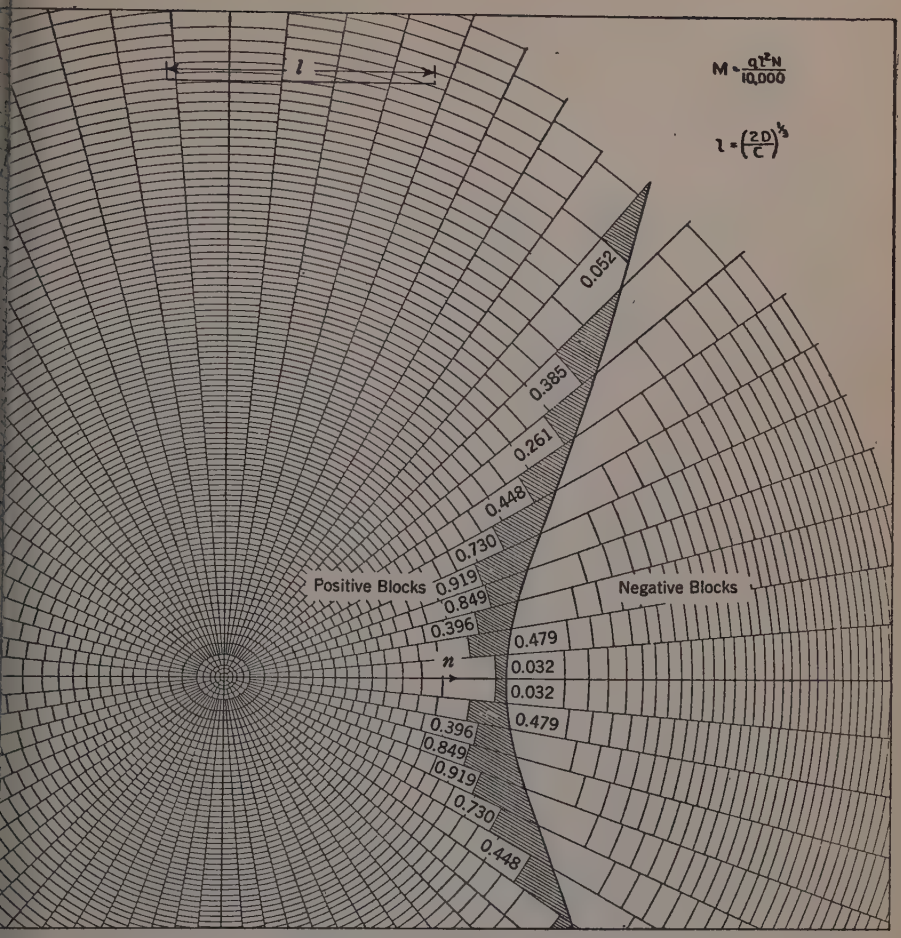

(b) Subgrade Assumed to Be an Elastic Solid

TE PAVEMENT SLAB (N = NUMBER OF POSITIVE BLOCKS MINUS NUMBER OF NEGATIVE IO FOR CONCRETE, 0.15)

respect to x from a_1 to a_2, and with respect to y from b_1 to b_2. From the resulting expressions, Tables 2(b) and 3(b) were computed. The charts of Fig. 4 were constructed from these tables. Expressions were put in the form:

$$M_x = M\,(a_2, b_2) - M\,(a_1, b_2) - M\,(a_2, b_1) + M\,(a_1, b_1) \ldots\ldots (12)$$

The general term on the right side of Eq. 12—$M\,(a, b)$—depends on which equation was used for deflection. For Eqs. 4 and 5, the result can be written

as follows:

$$M(a,b) = \frac{2\,q\,l^2}{\pi} \int_0^\infty \frac{\gamma^2 \sin\frac{\alpha\,a}{l}\left[S\left(1-\cos\frac{\beta\,b}{l}\,e^{-\gamma b/l}\right) - T\sin\frac{\beta\,b}{l}\,e^{-\gamma b/l}\right]}{\alpha(\beta^2+\gamma^2)\,[1+4\,(1-\mu)\,\alpha^2\,\gamma^2-(1-\mu)^2\,\alpha^4]}\,d\alpha \ldots (13)$$

in which, for Eq. 5,

$$S = \left\{(1-\mu)\,\alpha^2\,(A+2\,B\,\beta^2) - \mu\left[2\,A\,\beta^2 - B + l^2\frac{\partial^2}{\partial c^2}\,(A+2\,B\,\beta^2) + \frac{2\,l}{\gamma}\,(\gamma^2+\beta^2)\,\frac{\partial A}{\partial c}\right]\right\} \ldots (14a)$$

and

$$T = \left\{(1-\mu)\,\alpha^2\,(-2\,A\,\beta^2+B) - \mu\left[A+2\,B\,\beta^2 + l^2\frac{\partial^2}{\partial c^2}\,(-2\,A\,\beta^2+B) + \frac{2\,l}{\gamma}\,(\gamma^2+\beta^2)\,\frac{\partial B}{\partial c}\right]\right\} \ldots (14b)$$

CHART 6

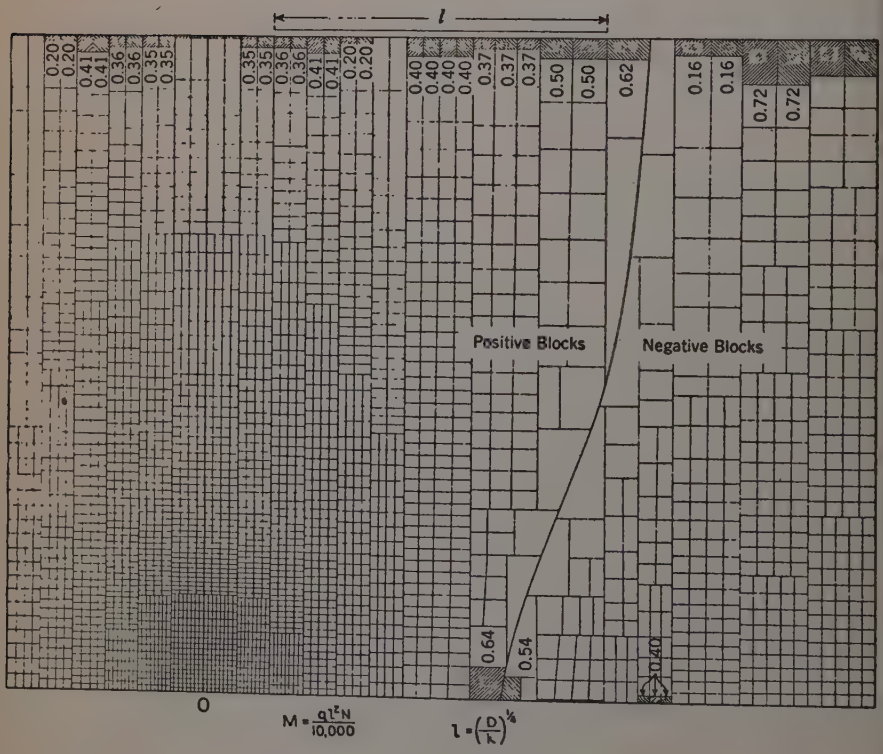

(*a*) At the Edge

FIG. 4.—INFLUENCE CHARTS FOR THE MOMENT $M = \frac{q\,l^2\,N}{10{,}000}$, AT POINT O ($N$ = NUMBER OF SHADED BLOCKS COUNT

and, for Eq. 4 (that is, for $c = 0$),

$$S = (1 - \mu^2)\,\alpha^2\,[1 + 2\,(1 - \mu)\,\alpha^2\,\beta^2] \quad \ldots\ldots\ldots\ldots (15a)$$

and

$$T = (1 - \mu^2)\,\alpha^2\,[(1 - \mu)\,\alpha^2 - 2\,\beta^2] \quad \ldots\ldots\ldots\ldots (15b)$$

In the evaluation of the integrals (of which the one in Eq. 13 is representative), the integrands were divided into two parts as previously explained.

Poisson's Ratio

Poisson's ratio was assumed to be 0.15 for all the computations. This choice was made because it is the value generally used by Mr. Westergaard.

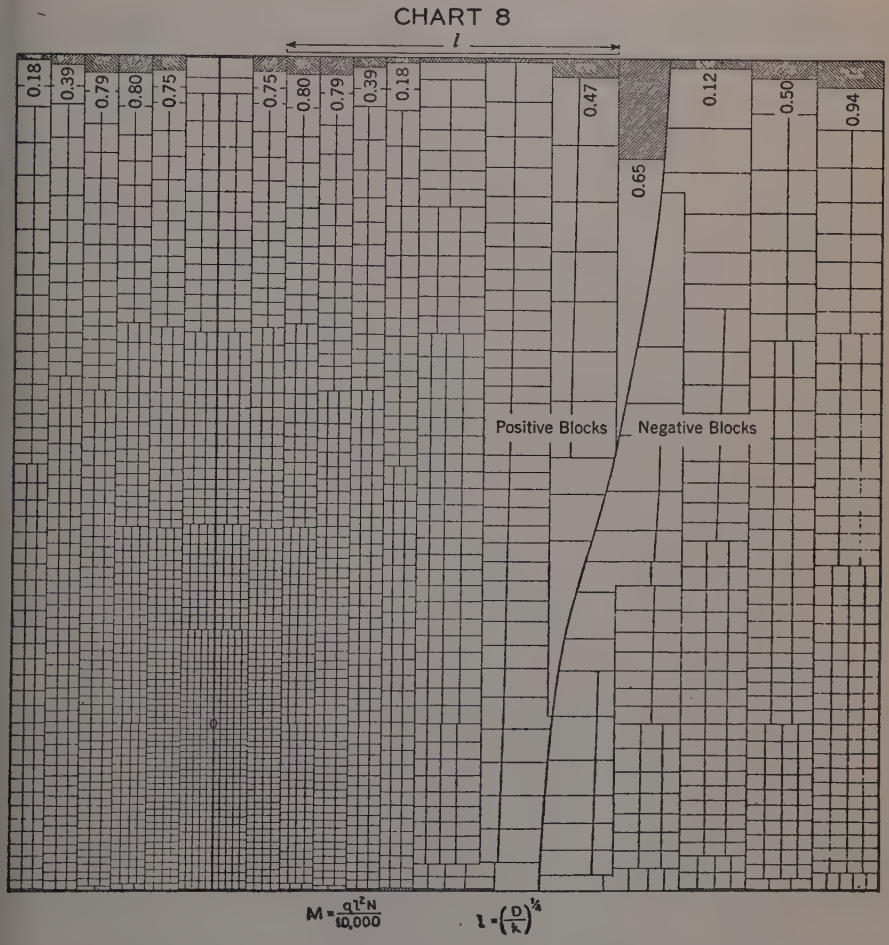

(*b*) Parallel to, and 0.5 *l*, from the Edge

Positive Blocks Minus Number of Negative Blocks; Poisson's Ratio for Concrete, 0.15; and Only as Fractions)

INTERIOR-LIQUID SUBGRADE

DEFLECTION

$$w = \frac{q l^4}{D} \frac{\theta_2 - \theta_1}{2\pi} \left[1 + \frac{\pi}{2} \frac{a}{l} \operatorname{Im} \sqrt{i}\, H_1^1\left(\frac{\sqrt{i}\, a}{l}\right) \right]$$

Formula for Table 1a –

$$\frac{2000\, w D}{q l^4} = 2000 \frac{(\theta_2 - \theta_1)}{2\pi} \left[1 + \frac{\pi a}{2 l} \operatorname{Im} \sqrt{i}\, H_1^1\left(\frac{\sqrt{i}\, a}{l}\right) \right]$$

MOMENT

$$M = \frac{q l}{8} \operatorname{Re} \left[(1+\mu)(\theta_2 - \theta_1) \frac{a}{l} \sqrt{i}\, H_1^1\left(\frac{\sqrt{i}\, a}{l}\right) + (1-\mu)(\sin 2\theta_2 - \sin 2\theta_1) \left\{ \frac{a}{2l} \sqrt{i}\, H_1^1\left(\frac{\sqrt{i}\, a}{l}\right) + H_1^1\left(\frac{\sqrt{i}\, a}{l}\right) - 0.5 \right\} \right]$$

Formula for Table 4a –

$$\frac{10000\, M}{q l^2} = \operatorname{Re} \left[125.4455 + \theta_1 \frac{a\sqrt{i}}{l} H_1^1\left(\frac{\sqrt{i}\, a}{l}\right) + 2\theta_1 H_1^1\left(\frac{\sqrt{i}\, a}{l}\right) - \theta_1 \right]$$

where $\theta_1 = 531.25 (\sin 2\theta_2 - \sin 2\theta_1)$

INTERIOR-SOLID SUBGRADE

DEFLECTION

$$w = \frac{q l^4}{D} \pi \sum_m (-1)^m \left[\frac{8}{3\sqrt{3}} \frac{\left(\frac{a}{2l}\right)^{6m+2}}{[(3m)!]^2 (6m+2)} + \frac{\frac{4}{\pi} \log \frac{\lambda a}{2l} - \frac{1}{6m+4} - \left(1 + \frac{1}{2} + \cdots + \frac{1}{3m+1}\right)}{[(3m+1)!]^2 (6m+4)} \left(\frac{a}{2l}\right)^{6m+4} - \frac{8}{3\sqrt{3}} \frac{\left(\frac{a}{l}\right)^{6m+6}}{[(3m+2)!]^2 (6m+6)} + \frac{2\left(\frac{a}{2l}\right)^{6m+7}}{[\Gamma(3m+3.5)]^2 (6m+7)} \right]$$

Formula for Table 1b

$$\frac{2000\, w D}{q l^4} = \pi \left(\frac{a}{l}\right)^2 \left[.1924501 + \left\{ .0458734 \left(\frac{a}{l}\right)^2 - .497759 \times 10^{-6} \left(\frac{a}{l}\right)^8 \right\} \log_{10} \left(\frac{a}{l}\right) - .0271743 \left(\frac{a}{l}\right)^2 - 1.002344 \times 10^{-3} \left(\frac{a}{l}\right)^4 + .202100 \times 10^{-3} \left(\frac{a}{l}\right)^5 - .2088217 \times 10^{-4} \left(\frac{a}{l}\right)^6 + .496338 \times 10^{-6} \left(\frac{a}{l}\right)^8 + .2175 \times 10^{-6} \left(\frac{a}{l}\right)^{10} - .2266 \times 10^{-9} \left(\frac{a}{l}\right)^{11} + .12948 \times 10^{-10} \left(\frac{a}{l}\right)^{12} \right]$$

MOMENT

$$M = \frac{q l^2}{16} \left[\sum_m \frac{(-1)^m \frac{8}{3\sqrt{3}} \left(\frac{a}{2l}\right)^{6m}}{[(3m)!]^2} \left\{ (1+\mu)(\theta_2 - \theta_1)6m + (1+\mu)(\sin 2\theta_2 - \sin 2\theta_1)(3m-1) \right. \right.$$

$$+ \sum_m \frac{(-1)^m 4 \left(\frac{a}{2l}\right)^{6m+2}}{\pi [(3m+1)!]^2} \left\{ (1+\mu)(\theta_2 - \theta_1) + \frac{1}{2}(1-\mu)(\sin\theta_2 - \sin\theta_1) + [(6m+2)(1+\mu)(\theta_2 - \theta_1) + 3m(1-\mu)(\sin\theta_2 - \sin\theta_1)] \left[\log \frac{\lambda a}{2l} - \left(1 + \frac{1}{2} + \cdots + \frac{1}{3m+1}\right) \right] \right\}$$

$$\left. - \sum_m \frac{(-1)^m \frac{8}{3\sqrt{3}} \left(\frac{a}{2l}\right)^{6m+4}}{[(3m+2)!]^2} \left\{ (6m+4)(1+\mu)(\theta_2 - \theta_1) + (3m+1)(1-\mu)(\sin 2\theta_2 - \sin 2\theta_1) \right\} + \sum_m \frac{(-1)^m 2 \left(\frac{a}{2l}\right)^{6m+5}}{[\Gamma(3m+3.5)]^2} \left\{ (6m+5)(1+\mu)(\theta_2 - \theta_1) + \frac{1}{2}(6m+3)(1-\mu)(\sin 2\theta_2 - \sin 2\theta_1) \right\} \right]$$

Formula for Table 4b

$$\frac{10000\, M}{q l^4} = A \log_{10} \frac{a}{l} + B\left(\frac{a}{l}\right)^2 + C\left(\frac{a}{l}\right)^4 + D\left(\frac{a}{l}\right)^5 + E\left(\frac{a}{l}\right)^6 + F\left(\log_{10} \frac{a}{l} + G\right)\left(\frac{a}{l}\right)^8 + H\left(\frac{a}{l}\right)^{10} + I\left(\frac{a}{l}\right)^{11} + J\left(\frac{a}{l}\right)^{12} + K\left(\log_{10} \frac{a}{l} + L\right)\left(\frac{a}{l}\right)^{14}$$

where

$A = -18.3887 (\theta_2 - \theta_1)$ $\quad$ $E = .0502958 (\theta_2 - \theta_1) + .709994\, \Theta_2$ $\quad$ $I = 1.62595 \times 10^{-4} (\theta_2 - \theta_1) + 28.1689 \times 10^{-4} \Theta_2$

$B = 4.91890 (\theta_2 - \theta_1) - 84.5511\, \Theta_2$ $\quad$ $F = 1.99530 \times 10^{-3} (\theta_2 - \theta_1) + 31.6873 \times 10^{-3} \Theta_2$ $\quad$ $J = -.109149 \times 10^{-4} (\theta_2 - \theta_1) - 1.92598 \times 10^{-4} \Theta_2$

$C = 1.207100 (\theta_2 - \theta_1) + 12.77989\, \Theta_2$ $\quad$ $G = -1.79745 \times 10^{-3} (\theta_2 - \theta_1) - 27.9717 \times 10^{-3} \Theta_2$ $\quad$ $K = -1.23717 \times 10^{-5} (\theta_2 - \theta_1) - 22.4541 \times 10^{-5} \Theta_2$

$D = -.354937 (\theta_2 - \theta_1) - 4.50937\, \Theta_2$ $\quad$ $H = -13.0979 \times 10^{-4} (\theta_2 - \theta_1) - 221.873 \times 10^{-4} \Theta_2$ $\quad$ $L = 1.41704 \times 10^{-3} (\theta_2 - \theta_1) + 25.6026 \times 10^{-3} \Theta_2$

θ_1 and θ_2 are in degrees and $\Theta_2 = \sin 2\theta_2 - \sin 2\theta_1$

FIG. 5.—WORKING FORMULAS FOR USE IN PREPARATION OF TABULAR DATA FOR CHART CONSTRUCTION

No doubt relatively simple corrections for the effect of Poisson's ratio similar to those given by Mr. Westergaard[18] could be developed.

SUMMARY OF THE COMPUTATIONS

Working formulas for computing values in Tables 1 to 4, in accordance with the procedure recommended in this paper, are presented in Figs. 5 and 6.

[18] "New Formulas for Stresses in Concrete Pavements of Airfields," by H. M. Westergaard, *Transactions*, ASCE, Vol. 113, 1948, p. 437, Table 1.

Influence Charts and Their Construction

An influence surface is similar to an influence line in that its ordinate at any point A gives the effect at a fixed point B of a unit load applied at point A. Influence surfaces are applicable to "two-dimensional" problems whereas influence lines are applicable to "one-dimensional" structures, such as beams or trusses.

Assume that the space between an influence surface and its reference plane is divided into cells with vertical walls, each cell being of unit volume and having

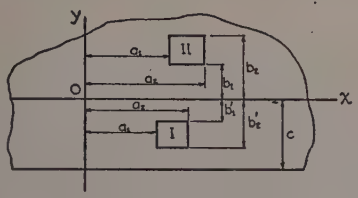

Boundaries of slab at $y=-c$ $y=+\infty$ $x=\pm\infty$

FOR LOAD ON REGION II

Deflection. $w_{II} = w_{II}(a_2,b_2) - w_{II}(a_1,b_2) - w_{II}(a_2,b_1) + w_{II}(a_1,b_1)$

Moment: $M_{II} = M_{II}(a_2,b_2) - M_{II}(a_1,b_2) - M_{II}(a_2,b_1) + M_{II}(a_1,b_1)$

FOR LOAD ON REGION I

Deflection: $w_I = w_I(a_2,b_2') - w_{II}(a_1,b_2') - w_I(a_2,b_1') + w_I(a_1,b_1')$

Moment: $M_I = M_I(a_2,b_2') - M_I(a_1,b_2') - M_I(a_2,b_1') + M_I(a_1,b_1')$

The general terms $w_{II}(a,b)$; $w_I(a,b)$; $M_{II}(a,b)$; $M_I(a,b)$ are as follows:

$w_{II}(a,b) = w'(a,b) - w''(a,b) + w'''(a,b)$; $\quad M_{II}(a,b) = M'(a,b) - M''(a,b) + M'''(a,b)$

$w_I(a,b) = w'(a,b') - w''(a,b') - w'''(a,-b) + w^{IV}(a,b')$; $\quad M_I(a,b) = M'(a,b') - M''(a,b') - M'''(a,-b') + M^{IV}(a,b')$

$$w'(a,b) = \frac{2q}{\pi k}\int_0^\infty \left[f_1(c)\left(1-e^{-\alpha b}\right) - f_2(c)\,\alpha\frac{b}{1}\,e^{-\alpha b}\right]\Theta \sin\alpha\frac{a}{1}\,\frac{d\alpha}{\alpha^2}\,;\quad M'(a,b) = \frac{2q\,l^2}{\pi}\int_0^\infty \left[f_3(c)\left(1-e^{-\alpha b}\right) - f_4(c)\,\alpha\frac{b}{1}\,e^{-\alpha b}\right]\Theta \sin\alpha\frac{a}{1}\,\frac{d\alpha}{\alpha}$$

$$w''(a,b) = \frac{2q}{\pi k}\left[\; f_1(c)\left\{0.4\,h_1(1.5,a,b) + 0.003\,h_1(0.44,a,b)\right\} - f_2(c)\left\{0.4\,h_2(1.5,a,b) + 0.003\,h_2(0.44,a,b)\right\}\right]$$

$$M''(a,b) = \frac{2q\,l^2}{\pi}\left[\; f_3(c)\left\{0.8\,h_3(1.5,a,b) + 0.006\,h_3(0.44,a,b)\right\} - f_4(c)\left\{0.8\,h_4(1.5,a,b) + 0.006\,h_4(0.44,a,b)\right\}\right]$$

$$w'''(a,b) = \frac{q}{\pi k}\sum\left[f_1(c) - \left\{f_1(c) + f_2(c)\alpha_n\frac{b}{1}\right\}e^{-\alpha_n\frac{b}{1}}\right]\frac{\Theta_n}{\alpha_n^2}\,(\alpha_{n+1}-\alpha_{n-1})\sin\alpha_n\frac{a}{1}\,;\quad M'''(a,b) = \frac{q\,l^2}{\pi}\sum\left[f_3(c) - \left\{f_3(c) + f_4(c)\alpha_n\frac{b}{1}\right\}e^{-\alpha_n\frac{b}{1}}\right]\Theta_n\,(\alpha_{n+1}-\alpha_{n-1})\sin\alpha_n\frac{a}{1}$$

$$w^{IV}(a,b) = \frac{q}{\pi k}\sum\left[g_1(n,c) - \left\{g_3(n,c)\cos\beta_n\frac{b}{1} + g_4(n,c)\sin\beta_n\frac{b}{1}\right\}e^{-\alpha_n\frac{b}{1}}\right]\psi_n\sin\alpha_n\frac{a}{1}$$

$$M^{IV}(a,b) = \frac{q\,l^2}{\pi}\sum\left[g_3(n,c) - \left\{g_3(n,c)\cos\beta_n\frac{b}{1} + g_4(n,c)\sin\beta_n\frac{b}{1}\right\}e^{-\alpha_n\frac{b}{1}}\right]\psi_n\sin\alpha_n\frac{a}{1}$$

$$w^{IV}(a,b') = \frac{q}{2\pi k}\sum\left[1-\cos\beta_n\frac{b'}{1}\cosh\gamma_n\frac{b'}{1} + \alpha_n^2\sin\beta_n\frac{b'}{1}\sinh\gamma_n\frac{b'}{1}\right]\left[\alpha_{n+1}-\alpha_{n-1}\right]\frac{\sin\alpha_n\frac{a}{1}}{\alpha_n(1+\alpha_n^4)}$$

$$M^{IV}(a,b') = \frac{q\,l^2}{2\pi}\sum\left[\alpha_n\left(1-\cos\beta_n\frac{b'}{1}\cosh\gamma_n\frac{b'}{1}\right) + (0.85\,\alpha_n^4 - 0.15)\sin\beta_n\frac{b'}{1}\sinh\gamma_n\frac{b'}{1}\right]\left[\alpha_{n+1}-\alpha_{n-1}\right]\frac{\sin\alpha_n\frac{a}{1}}{\alpha_n(1+\alpha_n^4)}$$

$$\Theta = \alpha(0.4\,e^{-1.5\alpha} + 0.003\,e^{-0.44\alpha})\,;\qquad \Theta_n = \alpha_n(0.4\,e^{-1.5\alpha_n} + 0.003\,e^{-0.44\alpha_n})\,;\qquad \psi_n = \frac{\gamma_n^2\,(\alpha_{n+1}-\alpha_{n-1})}{\alpha_n(\beta_n^4+\gamma_n^4)(1+3.4\,\alpha_n^2\,\gamma_n^2 - 0.7225\,\alpha_n^4)}$$

$$h_1(\delta,a,b) = \tan^{-1}\left(\frac{\delta+\frac{b}{1}}{\frac{a}{1}}\right) - \tan^{-1}\left(\frac{\delta}{\frac{a}{1}}\right)\,;\qquad h_2(\delta,a,b) = \frac{\frac{a}{1}\,\frac{b}{1}}{\left(\delta+\frac{b}{1}\right)^2 + \left(\frac{a}{1}\right)^2}$$

$$h_3(\delta,a,b) = \frac{a}{1}\left\{\frac{\delta}{\left[\delta^2+\left(\frac{a}{1}\right)^2\right]^2} - \frac{\left(\delta+\frac{b}{1}\right)}{\left[\left(\delta+\frac{b}{1}\right)^2+\left(\frac{a}{1}\right)^2\right]^2}\right\}\,;\qquad h_4(\delta,a,b) = \frac{a}{1}\,\frac{b}{1}\,\frac{3\left(\delta+\frac{b}{1}\right)^2 - \left(\frac{a}{1}\right)^2}{\left[\left(\delta+\frac{b}{1}\right)^2+\left(\frac{a}{1}\right)^2\right]^3}$$

When $c=0$ $\quad f_1(c)=1.425$; $\quad f_2(c)=0.425$; $\quad f_3(c)=1.3929375$, $\quad f_4(c)=0.4154375$

$g_1(n,c) = (1+1.7\,\alpha_n^2\,\beta_n^2)\,\psi_n$; $\qquad g_2(n,c) = (0.85\,\alpha_n^2 - 2\,\beta_n^2)\,\psi_n$,

$g_3(n,c) = 0.9775\,(1+1.7\,\alpha_n^2\,\beta_n^2)\,\alpha_n^2\,\psi_n$; $\qquad g_4(n,c) = 0.9775\,(0.85\,\alpha_n^4 - 2\,\beta_n^2)\,\alpha_n^2\,\psi_n$

When $c>0$ $\quad f_1(c)=0.669375$; $\quad f_2(c)=0.3346875$; $\quad f_3(c)=0.669375$; $\quad f_4(c)=0.28448375$

$$g_1(n,c) = \frac{1}{2}\left[1+3.4\,\beta_n^2\,\gamma_n^2 - 0.7225\,\alpha_n^4 + 2\,\alpha_n^2 q + \left\{1+0.7225\,\alpha_n^4 + 2g\sin 2\beta_n\frac{c}{1} - 2\alpha_n^2 g\cos 2\beta_n\frac{c}{1}\right\}e^{-2\gamma_n\frac{c}{1}}\right]$$

$$g_2(n,c) = 0.85\,\alpha_n^2 + 0.7225\,\beta_n^2\,\alpha_n^4 - \beta_n^2 + \left\{-0.7225\,\beta_n^2\,\alpha_n^4 - \beta_n^2 - g\alpha_n^2\sin 2\beta_n\frac{c}{1} + g\cos 2\beta_n\frac{c}{1}\right\}e^{-2\gamma_n\frac{c}{1}}$$

$$g_3(n,c) = \phi_n\left[d_3 + a_3\tan\beta_n\frac{c}{1}\left(1-\tanh\gamma_n\frac{c}{1}\right) + b_3\tanh\gamma_n\frac{c}{1} + c_3\tan^2\beta_n\frac{c}{1} + e_3\tan^2\beta_n\frac{c}{1}\tanh\gamma_n\frac{c}{1}\right]$$

$$g_4(n,c) = \phi_n\left[d_4 + a_4\tan\beta_n\frac{c}{1}\left(1-\tanh\gamma_n\frac{c}{1}\right) + b_4\tanh\gamma_n\frac{c}{1} + c_4\tan^2\beta_n\frac{c}{1} + e_4\tan^2\beta_n\frac{c}{1}\tanh\gamma_n\frac{c}{1}\right]$$

$\phi_n = \cos^2\beta_n\frac{c}{1}\,e^{-2\gamma_n\frac{c}{1}}\cosh\gamma_n\frac{c}{1}$; $\qquad d_3 = 0.9775\,(\alpha_n^2 + 1.7\,\beta_n^2\,\alpha_n^4)$; $\qquad a_3 = 2\,\alpha_n^2 q$; $\qquad b_3 = a_3 + e_3$,

$c_3 = a_4 + d_3$; $\qquad e_3 = (0.15 - 0.7225\,\alpha_n^4)(0.85\,\alpha_n^2 - 2\,\beta_n^2)$; $\qquad d_4 = 0.9775\,(0.85\,\alpha_n^4 - 2\,\beta_n^2\,\alpha_n^2)$

$a_4 = (0.85\,\alpha_n^4 - 0.15)\,2g$; $\qquad b_4 = e_4 - a_3$; $\qquad c_4 = f_4 - a_3$, $\qquad e_4 = (0.7225\,\alpha_n^4 - 0.15)\,(1 + 1.7\,\alpha_n^2\,\beta_n^2)$

$$q = 1.275\,\alpha_n^2 - \gamma_n^2 + \frac{0.15\,\alpha_n^2\,(2\,\gamma_n^2 - 0.85\,\alpha_n^2)}{2\,(\gamma_n^2+\beta_n^2)}\qquad \gamma_n = \sqrt{\frac{\sqrt{\beta_n^4+\alpha_n^4}+\alpha_n^2}{2}}\qquad \beta_n = \sqrt{\frac{\sqrt{\beta_n^4+\alpha_n^4}-\alpha_n^2}{2}}$$

Fig. 6.—Formulas for Deflections at Point O (Inset) and for Moments in the x-Direction at Point O, Due to a Uniform Unit Load q Over Regions I and II

as its base an element of the area of the reference plane. The reference plane thus divided into elemental areas would be an influence chart. An influence chart, therefore, represents the integral of the volume between an influence surface and its reference plane. Influence surfaces and influence charts, therefore, give answers to the same problems but in different form. Influence surfaces are better for showing the effects of concentrated loads but influence charts are preferable for showing the effects of distributed loads.

As indicated previously, each chart in this paper was constructed from a table of computed values. For example, Table 1(a) shows that for chart 1 the arc with a radius of 0.1012 l encloses two blocks in the first quadrant or one block for each 45° of arc. In Eq. 7, if $\pi/2$ is substituted for $\theta_2 - \theta_1$, and 0.1012 is substituted for a/l, $\frac{2{,}000\ w\ D}{q\ l^4} = 2$, the number of blocks enclosed. (For values of a/l greater than unity, published tables of Hankel functions were used; but, for smaller values of a/l, more accurate values than could be obtained from the tables were found by using the first terms of the series expansion of these functions.)

Likewise, in the right side of the formula for Table 4(a) given in Fig. 5, if 0 is substituted for θ_1, 5° (expressed in radians) for θ_2, and 0.1535 for a/l, the value of 2 is obtained. Had 0.2011 been substituted for a/l, the value of 3 would have been obtained. Thus, for chart 5 between radial lines of 0° and of 5°, and between the two arcs with radii of 0.1535 and 0.2011 (two consecutive values in Col. 1 of Table 4(a)), there is exactly one (3 − 2) full block.

Since practically every line in charts 1, 2, 3, and 4 is located by values given in Tables 1 and 4, the construction of these charts was relatively simple. The construction of charts 5, 6, 7, and 8 from Tables 2 and 3 is not so clearly indicated. These tables give the number of blocks per unit of area for specified areas of the influence charts. This information corresponds to that given by an influence surface since the value given when reduced to proper scale is the average ordinate of the corresponding influence surface over the specified area.

As an example of the information given by these tables, Table 2(a) denotes that, for the region between $b = 1.8\ l$, $b = 2.0\ l$, $a = 0$, and $a = 0.1\ l$ of chart 5, there must be 1.086 blocks per 0.01 l^2 of area, or a total of 2.172 blocks. In the construction of charts 5, 6, 7, and 8, care was exercised so that not only did each region have the correct number of blocks, but each block had the proper area for its position within the chart. This result was accomplished by interpolation.

Use of the Influence Charts

The use of the influence charts is demonstrated by the following examples:

It is required to find the stress at point O on a free edge of an 18-in. concrete pavement slab due to a load of 133,000 lb on a landing gear with twin wheels in tandem placed as shown in Fig. 7. Use the assumption of a dense liquid subgrade.

The essential data are: The lateral tire spacing is 31.5 in. and the fore and aft spacing is 62.0 in. Also, the tire pressure is 140 lb per sq in.; the modulus

of elasticity of concrete is 4,000,000 lb per sq in.; Poisson's ratio for the concrete is 0.15; and k, the modulus of the subgrade reaction, is 200 lb per cu in.

First, l, the radius of relative stiffness, must be determined. From the equation—

$$l = \sqrt[4]{\frac{E\,h^3}{12\,(1-\mu^2)\,k}} \qquad (16)$$

—l = 56.16 in. Next the tire imprint dimensions must be determined. The total imprint is equal to the wheel load divided by the tire pressure, or 33,250/140 = 237.5 sq in. Using an imprint outline of a rectangle with semicircular ends such that the width is equal to six tenths of the length, the following dimensions are computed: Length = 21.32 in. and width = 12.79 in. A tire imprint tracing is then drawn using the graphical scale shown on the proper chart (in this case, chart 6) and the tracing is superimposed on chart 6 with the wheels in the position indicated in the foregoing requirement, point O of tracing over point O of chart. Fig. 8 shows a part of chart 6 with an outline of the twin tandem tire prints placed as required.

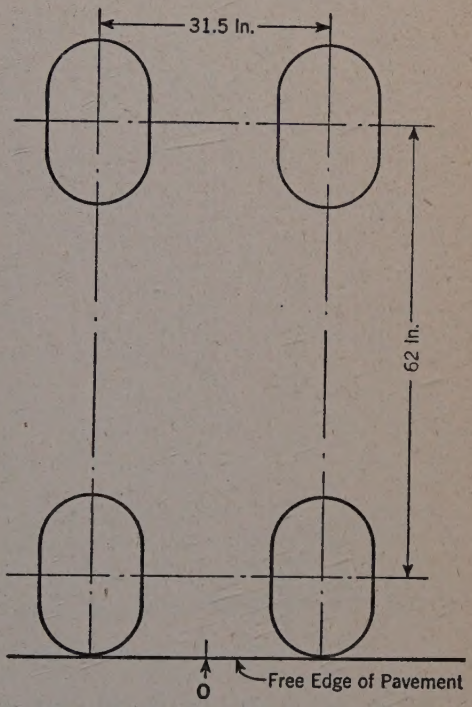

FIG. 7.—TWIN TANDEM LANDING GEAR AT THE EDGE OF A PAVEMENT

The number of blocks enclosed in each tire area is then determined by first counting all whole blocks and estimating all fractional blocks within the imprint area. In this case, the total number of blocks in all four tire prints is 439.2. Notice that the chart is symmetrical about the vertical axis so that, in this problem, it is necessary to count only the blocks in the two tire prints to the right of point O and to multiply the result by two.

Moment M is computed by the formulas given in the caption of each figure. The formula for chart 6 is $M = \frac{q\,l^2\,N}{10{,}000}$. Since q = 140, l = 56.16, and N = 439.2, $M = \frac{140 \times (55.16)^2 \times 439.2}{10{,}000}$, or 19,393 in.-lb.

The flexural stress can now be determined by multiplying the moment by the section modulus of the slab, $\frac{6}{h^2}$. Therefore, the stress at point O on a free edge of an 18-in. slab = $\frac{6 \times 19{,}393}{(18)^2}$, or 359.1 lb per sq in.

The stress may be obtained at point O with the tire imprint placed anywhere on the chart. The location of a load that gives maximum possible stress at the edge of a slab may be found by placing the wheel imprint tracing in different positions on the chart and counting the enclosed blocks in each position.

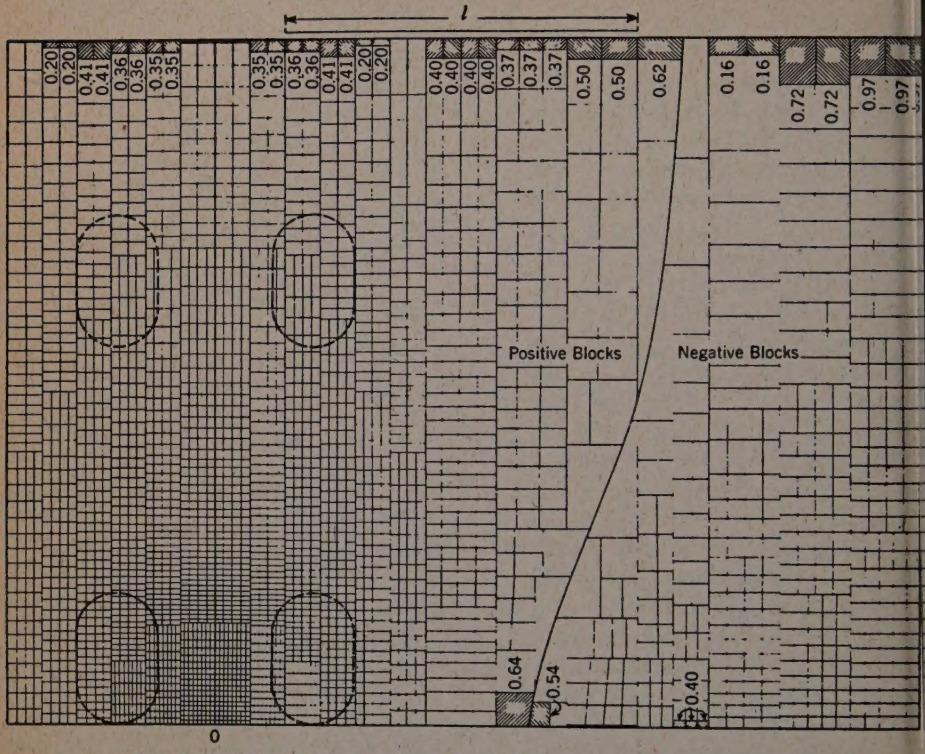

FIG. 8.—TRACING OF TWIN WHEELS IN TANDEM SUPERIMPOSED ON CHART 6

All charts are used in the same manner with the graphical scale and the formula given in the captions.

ACKNOWLEDGMENTS

This paper is the result of a cooperative project by the Engineering Experiment Station of Kansas State College at Manhattan and the Portland Cement Association at Chicago, Ill. The work was conducted under the direction of A. A. Anderson, Assoc. M. ASCE, of the Portland Cement Association and C. H. Scholer, M. ASCE, of Kansas State College. The writers wish to thank them for their assistance and encouragement.

E. J. Hennings worked on the project during the first few months, and gave valuable suggestions in regard to procedure. M. E. Raville shares equally with the writers the responsibility of directing and performing each detail of the project except the actual writing of this paper.

To W. C. Janes, credit is due for checking, correcting errors, and making valuable suggestions in regard to the mathematical derivations. F. J. McCormick Assoc. M. ASCE, made contributions to every phase of the work. To these and other contributors, the writers wish to express their thanks.

The paper was presented to the Air Transport Division at the Oklahoma City, Okla., meeting of the Society, on April 21, 1949.